FEBS Letters 586 (2012) 4088–4093

journal homepage: www.FEBSLetters.org

A comparative analysis of the aggregation behavior of amyloid-β peptide variants

Annelies Vandersteen [a,b,1], Ellen Hubin [a,c,d,1], Rabia Sarroukh [e], Greet De Baets [b], Joost Schymkowitz [b], Frederic Rousseau [b], Vinod Subramaniam [a], Vincent Raussens [e], Holger Wenschuh [f], Dirk Wildemann [f], Kerensa Broersen [a,*]

[a] Nanobiophysics Group, MIRA Institute for Biomedical Technology and Technical Medicine, Faculty of Science and Technology, University of Twente, 7500 AE Enschede, The Netherlands
[b] VIB Switch Laboratory, Department of Cellular and Molecular Medicine, Katholieke Universiteit Leuven (KUL), Herestraat 49 Box 802, 3000 Leuven, Belgium
[c] Structural Biology Brussels, Department of Biotechnology (DBIT), Vrije Universiteit Brussel (VUB), Pleinlaan 2, B-1050 Brussels, Belgium
[d] VIB Department of Structural Biology, Pleinlaan 2, B-1050 Brussels, Belgium
[e] Center for Structural Biology and Bioinformatics, Laboratory for Structure and Function of Biological Membranes, Université Libre de Bruxelles, CP 206/2 Blvd. du Triomphe, 1050 Brussels, Belgium
[f] JPT Peptide Technologies GmbH, Volmerstrasse 5 (UTZ), 12489 Berlin, Germany

ARTICLE INFO

Article history:
Received 5 July 2012
Revised 2 October 2012
Accepted 10 October 2012
Available online 24 October 2012

Edited by Jesus Avila

Keywords:
Thioflavin T fluorescence
Alzheimer's disease
FAD mutation
Biotinylation
p3 Peptide
Biophysics

ABSTRACT

Aggregated forms of the amyloid-β peptide are hypothesized to act as the prime toxic agents in Alzheimer disease (AD). The *in vivo* amyloid-β peptide pool consists of both C- and N-terminally truncated or mutated peptides, and the composition thereof significantly determines AD risk. Other variations, such as biotinylation, are introduced as molecular tools to aid the understanding of disease mechanisms. Since these modifications have the potential to alter key aggregation properties of the amyloid-β peptide, we present a comparative study of the aggregation of a substantial set of the most common *in vivo* identified and *in vitro* produced amyloid-β peptides.

Structured summary of protein interactions:
Amyloid beta and **Amyloid beta** bind by fluorescence technology (View Interaction: 1, 2, 3, 4, 5)
Amyloid beta and **Amyloid beta** bind by transmission electron microscopy (View Interaction: 1, 2)
Amyloid beta and **Amyloid beta** bind by filter binding (View Interaction: 1, 2, 3)

1. Introduction

Early aggregated forms of the amyloid-β peptide (Aβ), which is generated from the amyloid precursor protein (APP), have been considered the basis for development of Alzheimer's disease (AD) [1,2]. Despite extensive research, the exact link between Aβ and AD remains elusive. One of the underlying reasons is that APP processing *in vivo* does not generate a single, well-defined species. The main cause for peptide heterogeneity stems from the identification of two main APP processing pathways, termed 'non-amyloidogenic' and 'amyloidogenic'. The non-amyloidogenic pathway involves APP cleavage by α- and γ-secretase and generates the p3 peptide, an N-terminally truncated form of Aβ, while the amyloidogenic pathway releases Aβ by action of β- and γ-secretase [3]. Besides the dual processing of APP generating either p3 or Aβ, the γ-secretase cleavage site is ill-defined resulting in variation at the C-terminus of Aβ [4,5]. As a result thereof, released Aβ peptides vary in length from 27 to 49 amino acids [6,7]. Additional variation in the *in vivo* Aβ pool is attained by mutations within the Aβ domain of APP. Known mutations inducing familial AD (FAD) include the Flemish (Ala21 to Gly), Dutch (Glu22 to Gln), Italian (Glu22 to Lys), Arctic (Glu22 to Gly), Iowa (Asp23 to Asn), and Tottori (Asp7 to Asn) mutations (reviewed by [8]). An additional source of peptide variation results from the introduction of biotinylation as a research tool for interaction studies [9–12]. All modifications described above could affect peptide behavior due to altered aggregation properties. In this study we systematically compared the aggregation behavior of p3 and Aβ peptides resulting from heterogeneous APP processing as well as a selection of FAD-associated Aβ mutants and biotinylated variants.

* Corresponding author. Address: Nanobiophysics Group (NBP), University of Twente, Zuidhorst ZH155, 7500 AE Enschede, The Netherlands. Fax: +31 534891105.
E-mail address: k.broersen@utwente.nl (K. Broersen).
[1] These authors contributed equally to this work.

0014-5793/$36.00
http://dx.doi.org/10.1016/j.febslet.2012.10.022

2. Materials and methods

2.1. Aβ peptide synthesis

Aβ and p3 peptides were produced by JPT (JPT Peptide Technologies, Germany). Details on peptide synthesis and analysis of peptide identity and purity are described in SI.

2.2. Solubilization of Aβ peptides

Peptides were dissolved according to the standard procedure developed and validated in our laboratory [13]. In short, Aβ peptides were dissolved in 1,1,1,3,3,3-hexafluoro-2-propanol (HFIP). HFIP was evaporated using nitrogen gas and the peptide film was redissolved using dimethyl sulfoxide (DMSO). The peptide was separated from DMSO by elution from a HiTrap™ desalting column (GE Healthcare, cat. # 17-1408-01) into a 50 mM Tris pH 7.5 buffer containing 1 mM disodium ethylene-diaminetetraacetate (EDTA). The resulting samples were kept on ice until experiments started with a maximum lag time of 30 min. Peptide concentration was determined using the Coomassie (Bradford) Protein Assay kit and diluted to 25 μM in 50 mM Tris pH 7.5 buffer containing 1 mM EDTA. Incubation of Aβ peptides occurred for the given time periods at 25 °C under quiescent conditions. This procedure was slightly adapted for the ATR-FTIR samples and is described in SI.

2.3. Thioflavin T fluorescence

Aβ concentrations were adjusted to 1 μM using 50 mM Tris pH 7.5 buffer containing 1 mM EDTA and a final concentration of 12 μM Thioflavin T (ThT). The fibrillation kinetics of the various Aβ preparations were monitored *in situ* in a Greiner 96-well plate using a FLUOstar OPTIMA fluorescence plate reader (BMG LABTECH GmbH, Germany) at an excitation wavelength of 440 nm and an emission wavelength of 480 nm. Fluorescence readings were recorded every 5 min for a period of 20 h. Measurements were performed as independent triplicates. Recorded values were averaged and background measurements (buffer containing 12 μM ThT) were subtracted.

2.4. Transmission electron microscopy

After 2 weeks of incubation, Aβ aliquots (5 μL) were adsorbed to carbon-coated Formvar 400-mesh copper grids (Agar Scientific, cat. # S162-4) for 1 min. The grids were blotted, washed, and stained with 1% (wt/vol) uranyl acetate. Samples were studied with a JEOL JEM-1400 microscope (JEOL Ltd., Tokyo, Japan) at 80 kV. Images were collected from three independently prepared Aβ solutions.

2.5. Dotblot

After 0.5 h of incubation a volume of 5 μL Aβ was spotted onto a nitrocellulose membrane. The membranes were blocked in phosphate buffered saline containing 0.2% Tween-20 (1 h, 25 °C), and incubated (1 h, 25 °C) with primary A11 antibody (Invitrogen, cat. # AHB0052), diluted 1:4000 in 100 mM Hepes, pH 7.0 [14]. After incubation (0.5 h, 25 °C) with a secondary anti-rabbit-HRP-tagged antibody (Promega, cat. # W4011), diluted 1:5000 in phosphate buffered saline containing 0.05% Tween-20, the membranes were visualized using the Immobilon™ Western chemiluminescent HRP substrate system. Spots were manually selected and intensities of the spots were analyzed as mean grey values using ImageJ software [15]. Images were background subtracted.

2.6. Attenuated total reflectance-Fourier-transform infrared spectroscopy

ATR-FTIR spectra were recorded on an Equinox 55 IR spectrophotometer (Bruker Optics, Ettlingen, Germany). Two micrograms of Aβ was spread on the diamond surface (2×2 mm^2) of the internal reflection element (ERI) and was washed with excess milliQ water to eliminate salts. Excess water was evaporated under nitrogen flow. Each spectrum represents the mean of 128 repetitions, recorded at a resolution of 2 cm^{-1}. Details on data processing are described in SI.

2.7. Statistical Analysis

The intensities of A11-positive spots as determined with ImageJ software were further analyzed using the two-tailed unpaired t-test for significance. Significant differences are denoted $^*P < 0.05$.

3. Results

We present a comparison of the aggregation profiles of an extensive set of Aβ peptides with N- or C-terminal variation, FAD-related mutations, and biotinylated forms of Aβ. Aβ peptides were prepared by peptide synthesis. Identity and purity were confirmed by MALDI-TOF MS and LC–MS (Fig. S1–S4).

3.1. C-terminal elongation increases aggregation propensity and induces an amorphous fibrillar state

Aggregation kinetics of various Aβ lengths were recorded by ThT fluorescence and two different aggregation profiles could be distinguished: slow aggregation accompanied with long nucleation times and high final fluorescence intensity were detected for $A\beta_{1-37}$, $A\beta_{1-38}$ and $A\beta_{1-40}$, while $A\beta_{1-42}$ and $A\beta_{1-43}$ aggregated rapidly with almost immediate onset resulting in low final fluorescence intensity (Fig. 1A,B). Fibril morphology has been related to different affinities for ThT binding affecting the extent of ThT fluorescence intensity [16,17]. Visualization of fibrils by TEM indeed revealed morphologically distinct aggregates, showing extended negatively-stained fibrils for $A\beta_{1-37}$, $A\beta_{1-38}$ and $A\beta_{1-40}$, and heavily intertwined networks for $A\beta_{1-42}$ and $A\beta_{1-43}$ (Fig. 1C). Structural analysis by ATR-FTIR at early time points confirmed that these peptides adopted a β-sheet conformation, as seen by strong absorption at 1630 cm^{-1} (Fig. 1E). Apart from affecting fibril properties, increasing peptide length also leads to a more pronounced oligomerization as detected through dotblotting with the oligomer-specific A11 antibody (Fig. 1D). $A\beta_{1-37}$, $A\beta_{1-38}$ and $A\beta_{1-40}$ showed less oligomer accumulation after 0.5 h of incubation than $A\beta_{1-42}$ and $A\beta_{1-43}$. Accordingly, ATR-FTIR spectra observed for pre-fibrillar $A\beta_{1-42}$ and $A\beta_{1-43}$ suggested higher β-sheet content compared to oligomers produced from shorter Aβ peptides which appeared more as a mixture of β-sheet, random coil and α-helical secondary structure elements (Table 1). This confirms the earlier report that the conversion of monomeric Aβ peptide into oligomers and mature fibrils coincides with the accumulation of a β-sheet enriched conformation [18]. The shorter $A\beta_{1-37}$, $A\beta_{1-38}$ and $A\beta_{1-40}$ displayed a higher β-sheet index [calculated as the ratio of the (1695/1630 cm^{-1}) intensities] than the longer $A\beta_{1-42}$ and $A\beta_{1-43}$. This suggests a higher content of antiparallel β-strands which reflects a less extended conversion from the oligomeric, antiparallel conformation into the fibrillar, parallel conformation after 1.5 h of incubation [19].

3.2. FAD mutations affect the aggregation rate to various extents but have little effect on fibril morphology and secondary structure

Familial mutations of $A\beta_{1-42}$ displayed a short nucleation phase similar to that observed for wild type $A\beta_{1-42}$, but affected the rate

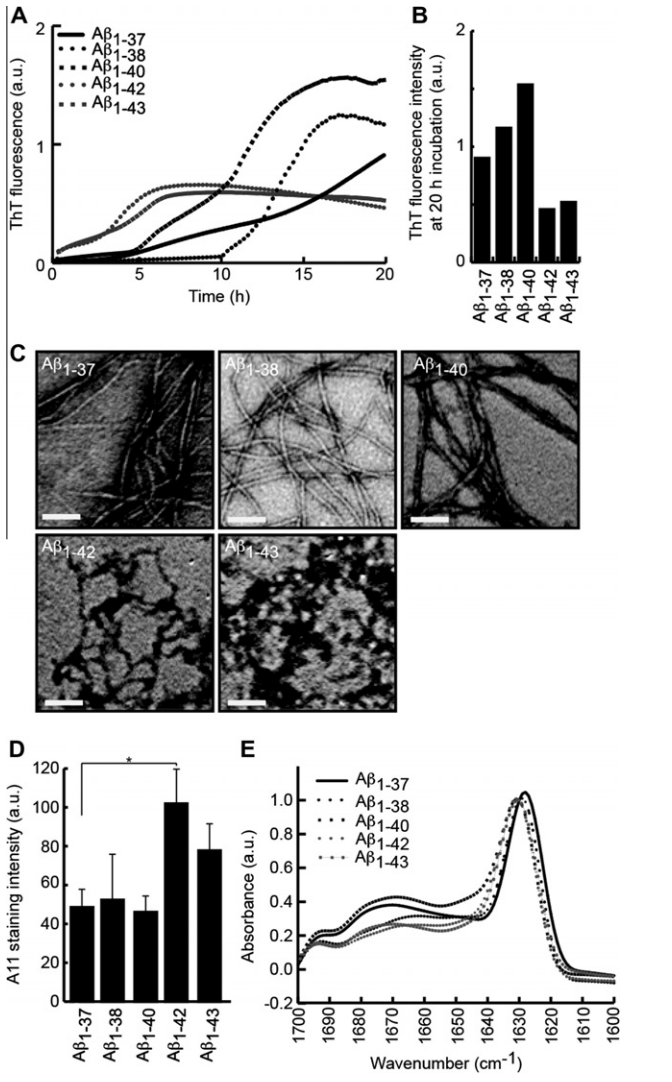

Fig. 1. Increased aggregation and oligomerization of Aβ with increasing peptide length. (A) Aggregation of C-terminal varying Aβ peptides monitored by ThT fluorescence. (B) ThT fluorescence intensities after 20 h of incubation. (C) TEM images of 2 weeks incubated Aβ at 25 °C. The scale bar represents 0.1 μm. (D) A11-reactivity of 0.5 h pre-incubated Aβ in a dotblot assay. (E) Deconvoluted ATR-FTIR spectra of Aβ peptides (2 μg) recorded after 1.5 h incubation at 25 °C.

of fibril elongation and final ThT fluorescence intensity (Fig. 2A,B). The slow polymerization of the D23N mutation coincided with a very low final ThT fluorescence, while A21G and E22Q mutations of $A\beta_{1-42}$ aggregated at a higher rate with an increased final ThT fluorescence intensity compared to wild type $A\beta_{1-42}$. All mutants of $A\beta_{1-42}$ displayed a β-sheet enriched conformation (Fig. 2E, Table 1) and eventually formed similar dense fibrillar networks (Fig. 2C). Oligomerization of the mutated $A\beta_{1-42}$ peptides showed little variability as seen by A11-reactivity (Fig. 2D), with exception of D23N $A\beta_{1-42}$, and β-sheet index analysis indicated similar oligomer-content for the various peptides (Table 1).

3.3. Biotinylation affects aggregation of $A\beta_{1-40}$ and $A\beta_{1-42}$

N- and C-terminal biotinylation of $A\beta_{1-40}$ increased the lag time of aggregation (Fig. 3A) while decreasing final ThT fluorescence (Fig. 3A,B), indicative of inhibited aggregation, without affecting fibril morphology (Fig. 3C). Oligomerization of biotinylated $A\beta_{1-40}$, as probed by A11-reactivity, was unaffected (Fig. 3D). Structural analysis of the peptides by ATR-FTIR however revealed absorption differences in the 1680–1640 cm^{-1} region (Fig. 3E, Table 1). Biotinylation of $A\beta_{1-42}$ reduced polymerization of the peptide compared to wild type $A\beta_{1-42}$ (Fig. 3A) without significantly affecting final ThT fluorescence (Fig. 3B), fibril morphology (Fig. 3C) or secondary structure content (Fig. 3E, Table 1). For $A\beta_{1-42}$ the impact of biotinylation on oligomerization depended on the location of the modification. C-terminal biotinylation did not affect A11-reactivity (Fig. 3D) but resulted in a reduced β-sheet index (Table 1). N-terminal modification on the other hand strongly impaired A11-reactivity (Fig. 3D) but did not influence the β-sheet index (Table 1). The β-sheet index of biotinylated peptides however needs to be interpreted with caution as the biotin tag might absorb around 1695 cm^{-1} leading to an overestimation of this value.

Table 1
Quantification of the secondary structure content using ATR-FTIR. Curve-fitting was performed on the non-deconvoluted FTIR spectra and resulted in estimated contributions of β-sheets (1613–1637 and 1682–1689 cm^{-1}), α-helices and random coil (1637–1662 cm^{-1}), and turns (1662–1682 cm^{-1}) to the secondary structure content of every Aβ peptide sample. The β-sheet index is defined as the ratio of the (1695 cm^{-1}/1630 cm^{-1}) intensities.

Secondary structure element(%)				
Peptide identity	β-Sheet	Random coil + α-helix	Turn	β-Sheet index
$A\beta_{1-37}$	36	44	20	0.28
$A\beta_{1-38}$	37	43	20	0.26
$A\beta_{1-40}$	47	33	20	0.27
$A\beta_{1-42}$	55	32	13	0.18
$A\beta_{1-43}$	56	28	16	0.14
D7N $A\beta_{1-42}$	55	30	15	0.19
A21G $A\beta_{1-42}$	51	33	16	0.22
E22G $A\beta_{1-42}$	41	37	22	0.18
E22K $A\beta_{1-42}$	45	39	16	0.16
E22Q $A\beta_{1-42}$	50	32	19	0.21
D23N $A\beta_{1-42}$	46	32	23	0.14
Biotin-$A\beta_{1-40}$	34	44	22	0.31
$A\beta_{1-40}$-K-biotin	42	39	19	0.21
Biotin-$A\beta_{1-42}$	54	34	12	0.17
$A\beta_{1-42}$-K-biotin	44	39	17	0.15
$p3_{17-40}$	39	41	20	0.25
$p3_{17-42}$	49	34	17	0.19

3.4. N-terminal truncation of Aβ induces rapid onset aggregation

Both N-terminally truncated forms of $A\beta_{1-40}$ and $A\beta_{1-42}$, $p3_{17-40}$ and $p3_{17-42}$ respectively, were characterized by rapid onset of aggregation compared to their corresponding full-length forms with decreased final ThT fluorescence intensity (Fig. 4A,B). From a morphological perspective, visualization by TEM revealed short fibrillar fragments for $p3_{17-40}$ dissimilar from the long extended networks observed for full-length $A\beta_{1-40}$ (Fig. 4C). Truncation of $A\beta_{1-42}$ to $p3_{17-42}$ only slightly affected fibril morphology resulting in less curly fibrils (Fig. 4C). Structural analysis by ATR-FTIR indicated that $p3_{17-40}$ displayed less β-sheets and more random coil and α-helical content than full-length $A\beta_{1-40}$. A similar observation was made for $p3_{17-42}$ compared to $A\beta_{1-42}$ (Fig. 3E, Table 1). Oligomerization of the truncated p3 peptides, as analyzed by A11-reactivity and the β-sheet index, was not significantly affected compared to the full-length counterparts (Fig. 4D, Table 1).

4. Discussion

The *in vivo* Aβ pool contains a high degree of variability, consisting of peptides with C-terminal variations, FAD-related mutations, and N-terminal truncations. To elucidate the mechanisms leading to Alzheimer disease (AD) some peptides have been additionally modified, *e.g.* biotinylated, to enable their investigation in experimental research. We chemically synthesized Aβ peptide variants

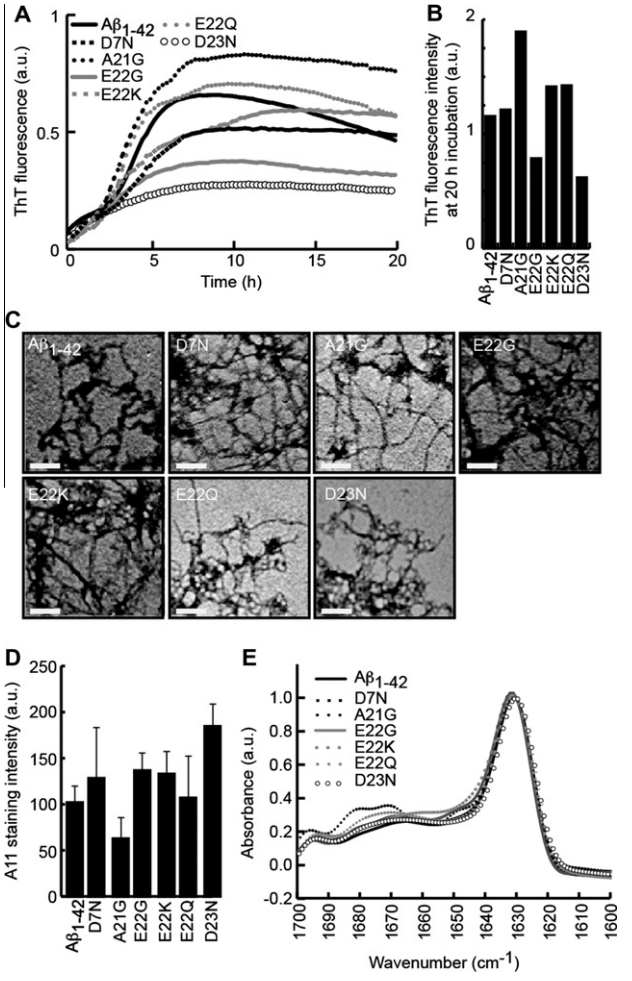

Fig. 2. Some FAD mutations affect aggregation and oligomerization of $A\beta_{1-42}$. (A) Aggregation of $A\beta_{1-42}$ FAD mutations monitored by ThT fluorescence. (B) ThT fluorescence intensities after 20 h of incubation. (C) TEM images of 2 weeks incubated Aβ at 25 °C. The scale bar represents 0.1 μm. (D) A11-reactivity of 0.5 h pre-incubated Aβ in a dotblot assay. (E) Deconvoluted ATR-FTIR spectra of Aβ peptides (2 μg) recorded after 1.5 h incubation at 25 °C.

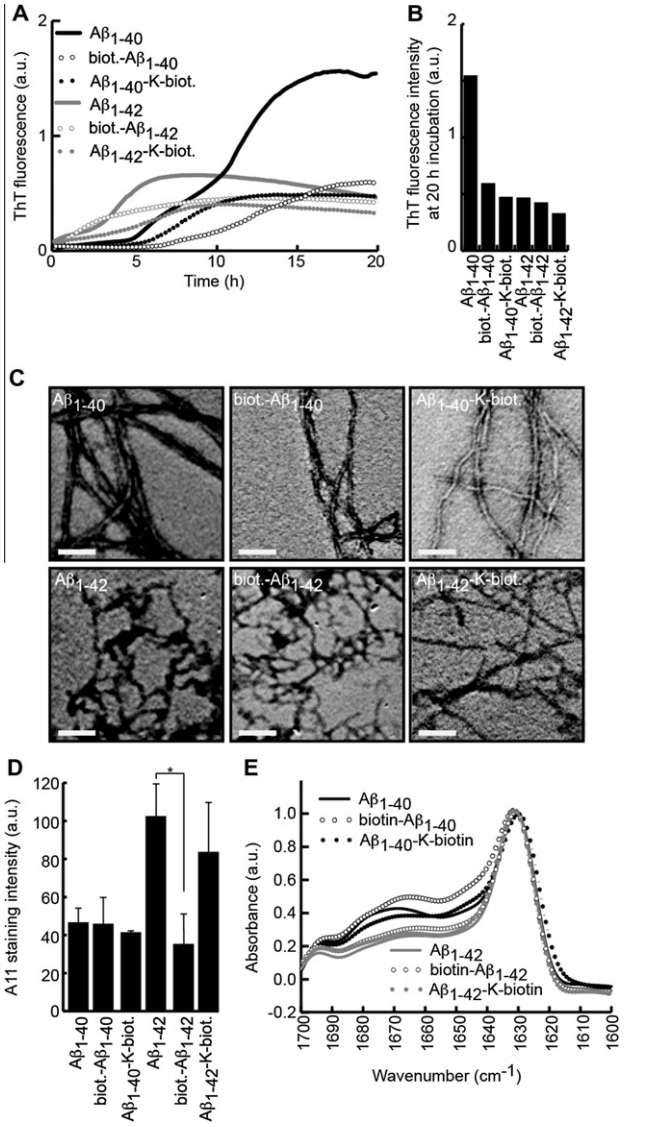

Fig. 3. C- and N-terminal biotinylation of $A\beta_{1-42}$ and $A\beta_{1-40}$ differentially affect aggregation. (A) Aggregation of C- and N-terminally biotinylated forms of $A\beta_{1-40}$ and $A\beta_{1-42}$ monitored by ThT fluorescence. (B) ThT fluorescence intensities after 20 h of incubation. (C) TEM images of 2 weeks incubated Aβ at 25 °C. The scale bar represents 0.1 μm. (D) A11-reactivity of 0.5 h pre-incubated Aβ in a dotblot assay. (E) Deconvoluted ATR-FTIR spectra of Aβ peptides (2 μg) recorded after 1.5 h incubation at 25 °C.

to compare their aggregation and oligomerization behaviors using biophysical techniques. Our observations show that variations in the Aβ sequence can have consequences for the propensity of the Aβ peptide to aggregate and oligomerize.

C-terminal variation was previously shown to affect aggregation propensity, and it has been generally reported that $A\beta_{1-42}$ aggregates at a higher rate than $A\beta_{1-40}$ [20,21]. Even though approximately 90% of the Aβ peptide pool is composed of these two peptides, it was recently recognized that also $A\beta_{1-37}$, $A\beta_{1-38}$, and $A\beta_{1-43}$ are present in the brain and may modulate disease progress [22]. We show that C-terminal extension generally results in faster aggregation and gradual transformation into densely networked β-sheet rich aggregates compared to shorter peptides, which form extended fibrils characterized by a primarily disordered structure. We further observed that $A\beta_{1-37}$ and $A\beta_{1-38}$ generally behave similar to $A\beta_{1-40}$ while the behavior of $A\beta_{1-43}$ strongly resembles that of $A\beta_{1-42}$. The dense fibril networks formed by $A\beta_{1-42}$ and $A\beta_{1-43}$ possibly provide less access to the ThT dye compared to the more extended fibrils of shorter peptides, resulting in a lower final ThT fluorescence intensity. Alternatively, the denser peptide networks can be more prone to precipitation in the test tube which would lead to a similar observation. Although the effect of FAD-related mutations of $A\beta_{1-42}$ on aggregation has been investigated in the past [23–26], no comprehensive study has been reported that directly compares the majority of the currently known mutations. Different Aβ preparation methods and experimental conditions have led to considerable variation in reported effects of these mutations. ThT fluorescence data in this study were measured at a physiologically relevant Aβ concentration of 1 μM. Most FAD-related mutations are located in or near the central hydrophobic cluster of the Aβ peptide, which has been predicted and reported to play an important role in aggregation [23,27–31]. FAD mutations can thus either inhibit or induce aggregation depending on the suitability of the replacing amino acid to accommodate an amyloidogenic or aggregated structure. Molecular dynamics simulations have suggested the depletion of the E22-K28 salt bridge to explain the enhanced aggregation of E22Q $A\beta_{1-42}$, while the switch of a bend motif to a turn in the region $A\beta_{22-28}$ could result in slower aggregation of the D23N $A\beta_{1-42}$ mutant [25]. Overall fibril morphology is however not affected, as has

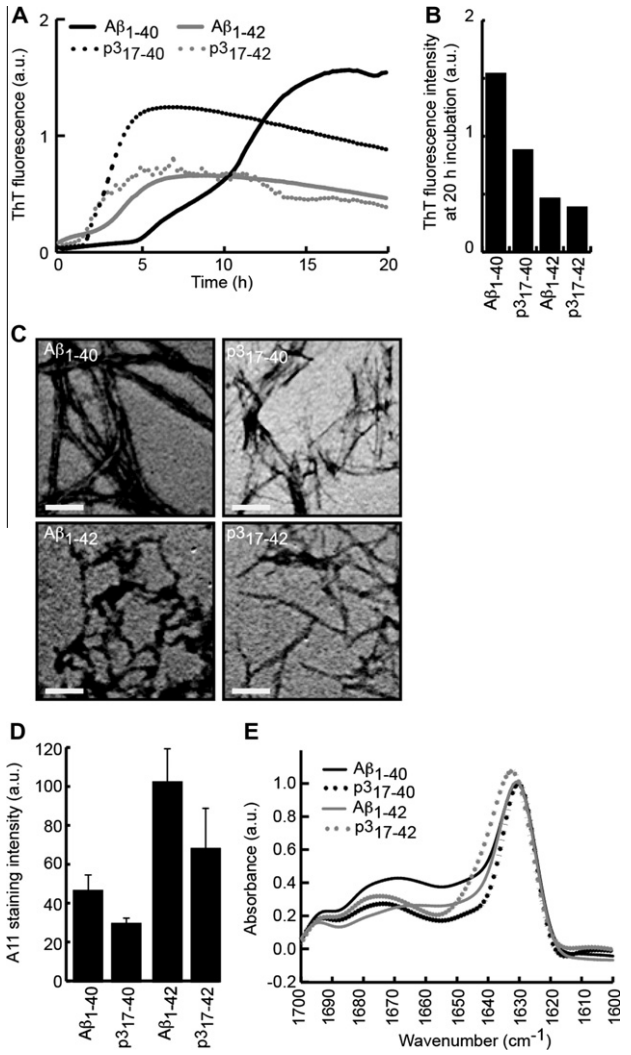

Fig. 4. p3 Peptides show pronounced aggregation. (A) Aggregation of $p3_{17-40}$ and $p3_{17-42}$ monitored by ThT fluorescence. (B) ThT fluorescence intensities after 20 h of incubation. (C) TEM images of 2 weeks incubated Aβ at 25 °C. The scale bar represents 0.1 μm. (D) A11-reactivity of 0.5 h pre-incubated Aβ in a dotblot assay. (E) Deconvoluted ATR-FTIR spectra of Aβ peptides (2 μg) recorded after 1.5 h incubation at 25 °C.

been shown previously for a subset of FAD mutants [23]. The central hydrophobic region is however not the absolute key in determining aggregation tendency as a subset of the FAD mutations in this region has no effect on the aggregation rate and most likely exert their pathological function through aberrant APP processing or reduced proteolytic Aβ degradation [32–34]. We further show that C-terminal elongation, which does not affect the central region of Aβ, also affects aggregation. Moreover, complete destruction of the central aggregation zone by deletion of the first 17 N-terminal amino acids, as naturally occurs by APP processing via the non-amyloidogenic pathway, does not abolish the aggregating character of the peptides, as was observed before [35] and upregulation of the α-secretase cleavage pathway initiating the non-amyloidogenic processing of APP has served as a template for the generation of various potential disease modulating drugs [36]. It is thus likely to suggest that, even though the central Aβ region can play a regulating role in the aggregation process, the C-terminal region may dominate this effect by determining fibril morphology. Biotinylation of Aβ has been applied in several studies [9–12]. Our data show that this modification can affect the onset of aggregation substantially depending on the type of biotinylation applied and its location, either N- or C-terminally, without affecting fibril morphology or oligomer formation. These observations underline the importance of selecting and validating the type of labeling required for experiments without inducing changes in the peptide behavior that are subject to study.

In this work we systematically compared a wide range of Aβ peptides for their aggregation properties. The overall aggregation profile was determined by thioflavin T fluorescence while we attempted to gain insight in early aggregation events by probing oligomerization of the peptides. We therefore used A11-reactivity as well as analysis of secondary structure content which were however not always completely in agreement. This could be attributed to the polyclonal nature of the A11 antibody [14] that can be hypothesized to recognize more than one conformation. On the other hand, it might be likely that both methods detect different oligomeric species. In conclusion, the results highlight that minor sequential variations may have consequences for the aggregation of Aβ.

Acknowledgments

AV and GDB were supported by a doctoral fellowship of the Agency for Innovation by Science and Technology Flanders (IWT), EH was supported by a doctoral fellowship of the Research Foundation Flanders (FWO) and KB was a recipient of the FWO Odysseus grant and is supported by UTWIST. RS and VR were supported by the National Fund for Scientific Research (FRNS).

Appendix A. Supplementary data

Supplementary data associated with this article can be found, in the online version, at http://dx.doi.org/10.1016/j.febslet.2012.10.022.

References

[1] Glenner, G.G. and Wong, C.W. (1984) Alzheimer's disease: initial report of the purification and characterization of a novel cerebrovascular amyloid protein. Biochem. Biophys. Res. Commun. 120, 885–890.
[2] Pike, C.J., Walencewicz, A.J. and Glabe, C.G. (1991) In vitro aging of beta-amyloid protein causes peptide aggregation and neurotoxicity. Brain Res. 563, 311–314.
[3] Nunan, J. and Small, D.H. (2000) Regulation of APP cleavage by alpha-, beta- and gamma-secretases. FEBS Lett. 483, 6–10.
[4] Weidemann, A., Eggert, S., Reinhard, F.B., Vogel, M., Paliga, K., Baier, G., Masters, C.L., Beyreuther, K. and Evin, G. (2002) A novel epsilon-cleavage within the transmembrane domain of the Alzheimer amyloid precursor protein demonstrates homology with Notch processing. Biochemistry 41, 2825–2835.
[5] Zhao, G., Mao, G., Tan, J., Dong, Y., Cui, M.-Z., Kim, S.-H. and Xu, X. (2004) Identification of a new presenilin-dependent zeta-cleavage site within the transmembrane domain of amyloid precursor protein. J. Biol. Chem. 279, 50647–50650.
[6] Vigo-Pelfrey, C., Lee, D., Keim, P., Lieberburg, I. and Schenk, D.B. (1993) Characterization of beta-amyloid peptide from human cerebrospinal fluid. J. Neurochem. 61, 1965–1968.
[7] Takami, M., Nagashima, Y., Sano, Y., Ishihara, S., Morishima-Kawashima, M., Funamoto, S. and Ihara, Y. (2009) Gamma-secretase: successive tripeptide and tetrapeptide release from the transmembrane domain of beta-carboxyl terminal fragment. J. Neurosci. 29, 13042–13052.
[8] Van Dam, D. and De Deyn, P.P. (2006) Drug discovery in dementia: the role of rodent models. Nat. Rev. Drug Discovery 5, 956–970.
[9] Bohrmann, B. et al. (1999) Endogenous proteins controlling amyloid beta-peptide polymerization. Possible implications for beta-amyloid formation in the central nervous system and in peripheral tissues. J. Biol. Chem. 274, 15990–15995.
[10] Leissring, M.A., Lu, A., Condron, M.M., Teplow, D.B., Stein, R.L., Farris, W. and Selkoe, D.J. (2003) Kinetics of amyloid beta-protein degradation determined by novel fluorescence- and fluorescence polarization-based assays. J. Biol. Chem. 278, 37314–37320.
[11] Liu, R., Barkhordarian, H., Emadi, S., Park, C. and Sierks, M. (2005) Trehalose differentially inhibits aggregation and neurotoxicity of beta-amyloid 40 and 42. Neurobiol. Dis. 20, 74–81.

[12] Nelson, T.J. and Alkon, D.L. (2007) Protection against beta-amyloid-induced apoptosis by peptides interacting with beta-amyloid. J. Biol. Chem. 282, 31238–31249.
[13] Broersen, K., Jonckheere, W., Rozenski, J., Vandersteen, A., Pauwels, K., Pastore, A., Rousseau, F. and Schymkowitz, J. (2011) A standardized and biocompatible preparation of aggregate-free amyloid beta peptide for biophysical and biological studies of Alzheimer's disease. Protein engineering, design & selection. PEDS 24, 743–750.
[14] Kayed, R., Head, E., Thompson, J.L., McIntire, T.M., Milton, S.C., Cotman, C.W. and Glabe, C.G. (2003) Common structure of soluble amyloid oligomers implies common mechanism of pathogenesis. Science 300, 486–489.
[15] Abramoff, M.D., Magalhaes, P.J. and Ram, S.J. (2004) Image processing with image. J. Biophotonics Int. 11, 36–42.
[16] Groenning, M. (2009) Binding mode of Thioflavin T and other molecular probes in the context of amyloid fibrils-current status. J. Chem. Biol. 3, 1–18.
[17] Biancalana, M. and Koide, S. (2010) Molecular mechanism of Thioflavin-T binding to amyloid fibrils. Biochim. Biophys. Acta 1804, 1405–1412.
[18] Barrow, C.J., Yasuda, A., Kenny, P.T. and Zagorski, M.G. (1992) Solution conformations and aggregational properties of synthetic amyloid beta-peptides of Alzheimer's disease. Analysis of circular dichroism spectra. J. Mol. Biol. 225, 1075–1093.
[19] Cerf, E., Sarroukh, R., Tamamizu-Kato, S., Breydo, L., Derclaye, S., Dufrêne, Y.F., Narataniaswami, V., Goormaghtigh, E., Ruysschaert, J. and Raussens, V. (2009) Antiparallel β-sheet: a signature structure of the oligomeric amyloid β-peptide. Biochem. J. 421, 415–423.
[20] Jarrett, J.T., Berger, E.P. and Lansbury, P.T. (1993) The carboxy terminus of the beta amyloid protein is critical for the seeding of amyloid formation: implications for the pathogenesis of Alzheimer's disease. Biochemistry 32, 4693–4697.
[21] Snyder, S.W., Ladror, U.S., Wade, W.S., Wang, G.T., Barrett, L.W., Matayoshi, E.D., Huffaker, H.J., Krafft, G.A. and Holzman, T.F. (1994) Amyloid-beta aggregation: selective inhibition of aggregation in mixtures of amyloid with different chain lengths. Biophys. J. 67, 1216–1228.
[22] Portelius, E., Bogdanovic, N., Gustavsson, M.K., Volkmann, I., Brinkmalm, G., Zetterberg, H., Winblad, B. and Blennow, K. (2010) Mass spectrometric characterization of brain amyloid beta isoform signatures in familial and sporadic Alzheimer's disease. Acta Neuropathol. 120, 185–193.
[23] Murakami, K., Irie, K., Morimoto, A., Ohigashi, H., Shindo, M., Nagao, M., Shimizu, T. and Shirasawa, T. (2003) Neurotoxicity and physicochemical properties of Abeta mutant peptides from cerebral amyloid angiopathy: implication for the pathogenesis of cerebral amyloid angiopathy and Alzheimer's disease. J. Biol. Chem. 278, 46179–46187.
[24] Baumketner, A., Krone, M.G. and Shea, J.E. (2008) Role of the familial Dutch mutation E22Q in the folding and aggregation of the 15–28 fragment of the Alzheimer amyloid-β protein. Proc. Natl. Acad. Sci. USA 105, 6027.
[25] Krone, M.G., Baumketner, A., Bernstein, S.L., Wyttenbach, T., Lazo, N.D., Teplow, D.B., Bowers, M.T. and Shea, J.E. (2008) Effects of familial Alzheimer's disease mutations on the folding nucleation of the amyloid beta-protein. J. Mol. Biol. 381, 221–228.
[26] Ono, K., Condron, M.M. and Teplow, D.B. (2010) Effects of the English (H6R) and Tottori (D7N) familial Alzheimer disease mutations on amyloid beta-protein assembly and toxicity. J. Biol. Chem. 285, 23186–23197.
[27] Fernandez-Escamilla, A.-M., Rousseau, F., Schymkowitz, J. and Serrano, L. (2004) Prediction of sequence-dependent and mutational effects on the aggregation of peptides and proteins. Nat. Biotechnol. 22, 1302–1306.
[28] Liu, R., McAllister, C., Lyubchenko, Y. and Sierks, M.R. (2004) Residues 17–20 and 30–35 of beta-amyloid play critical roles in aggregation. J. Neurosci. Res. 75, 162–171.
[29] Lopez-De la Paz, M.L., Goldie, K., Zurdo, J., Lacroix, E., Dobson, C.M., Hoenger, A. and Serrano, L. (2002) De novo designed peptide-based amyloid fibrils. Proc. Natl. Acad. Sci. USA 99, 16052–16057.
[30] Sánchez de Groot, N., Pallarés, I., Avilés, F.X., Vendrell, J. and Ventura, S. (2005) Prediction of "hot spots" of aggregation in disease-linked polypeptides. BMC Struct. Biol. 5, 18.
[31] Chiti, F., Stefani, M., Taddei, N., Ramponi, G. and Dobson, C.M. (2003) Rationalization of the effects of mutations on peptide and protein aggregation rates. Nature 424, 805–808.
[32] Tian, Y., Bassit, B., Chau, D. and Li, Y.M. (2010) An APP inhibitory domain containing the Flemish mutation residue modulates gamma-secretase activity for Abeta production. Nat. Struct. Mol. Biol. 17, 151–158.
[33] Betts, V., Leissring, M.A., Dolios, G., Wang, R., Selkoe, D.J. and Walsh, D.M. (2008) Aggregation and catabolism of disease-associated intra-Abeta mutations: reduced proteolysis of AbetaA21G by neprilysin. Neurobiol. Dis. 31, 442–450.
[34] Morelli, L., Llovera, R., Gonzalez, S.A., Affranchino, J.L., Prelli, F., Frangione, B., Ghiso, J. and Castano, E.M. (2003) Differential degradation of amyloid beta genetic variants associated with hereditary dementia or stroke by insulin-degrading enzyme. J. Biol. Chem. 278, 23221–23226.
[35] Pike, C.J., Overman, M.J. and Cotman, C.W. (1995) Amino-terminal deletions enhance aggregation of β-amyloid peptides in vitro. J. Biol. Chem. 270, 23895–23898.
[36] Fahrenholz, F. (2007) Alpha-secretase as a therapeutic target. Curr. Alzheimer Res. 4, 412–417.